

Applying artificial snowfalls to reduce the melting of the Muz Taw Glacier, Sawir Mountains

Feiteng Wang^{1*}, Xiaoying Yue¹, Lin Wang¹, Huilin Li¹, Zhencai Du², Jing Ming³,
Zhongqin Li¹

1 State Key Laboratory of Cryospheric Science / Tien Shan Glaciological Station, Northwest Institute of Eco-Environment and Resources, Chinese Academy of Sciences, Lanzhou 730000, China

2 Center for Monsoon System Research, Institute of Atmospheric Physics, Chinese Academy of Sciences, Beijing 100029, China

3 Beacon Science & Consulting, Doncaster East, VIC 3109, Australia

Correspondence

* Feiteng Wang, wangfeiteng@lzb.ac.cn

1 **ABSTRACT**

2 The glaciers in the Sawir Mountains, Altai area, have been experiencing a continuing
3 and accelerating ice loss since 1959, although the snowfall here is abundant and
4 evenly distributed over the year. As an attempt to reduce their melting, we carried
5 out two artificial-snowfall experiments to the Muz Taw glacier during 19 – 22 Aug
6 2018. We measured the albedo and mass balance at different sites along the glacier
7 before and after the experiments. Two automatic weather stations (AWS) were set
8 up at the equilibrium line altitude (ELA) of the glacier as the target area and the
9 forefield as the control area to record the precipitations, respectively. The
10 comparison of the two precipitation records from the two AWSs suggests that natural
11 precipitation could account for up to 21% of the snowfall received by the glacier
12 during the experiments. Because of the snowfalls, the glacier’s surface albedo
13 significantly increased in the mid-upper part; the average mass loss during Aug 18 –
14 24 (after the experiments) decreased by between 32 (14%) and 41 (17%) mm w.e.
15 comparing to that during Aug 12 – 18 (before the experiments); and the mass
16 resulting from the snowfalls accounted for between 42% and 54% of the total melt
17 during Aug 18 – 24. We also propose a mechanism involving artificial snowfall,
18 albedo and mass balance and the feedbacks, describing the role of snowfall in
19 reducing the melting of the glacier. The work in current status is primitive as a
20 preliminary trial, the conclusions of which need more controlling experiments to
21 validate in larger spatial and temporal scales in future.

22

23 **Keywords**

24 artificial snowfall, Muz Taw Glacier, Sawir Mountains, glacier mass balance, reduce
25 melting

26

27 **1 Introduction**

28 Mountain glaciers are an essential part of the cryosphere. As high-altitude reservoirs,
29 they are vital solid-water resources (Immerzeel et al., 2019; Immerzeel et al., 2010).
30 Glacier fluctuations represent an integration of changes in the mass and energy
31 balance and are well recognized as high-confidence indicators of climate change
32 (Bojinski et al., 2014). Satellite and in-situ observations of changes in the glacial
33 area, length and mass show a global coherence of continued mountain-glacier
34 recession in the last three decades with only a few exceptions (Zemp et al., 2019).
35 For the Sawir Mountains, the ablation of the glaciers is more intense than the global
36 average, and the total area of the glaciers reduced by 46% from 23 km² in 1977 to
37 12.5 km² in 2017 (Wang et al., 2019). The accelerated retreat of glaciers not only
38 causes spatial and temporal changes in water resources but also has a significant
39 impact on sea-level rise, regional water cycles, ecosystems and socio-economic
40 systems (such as agriculture, hydropower and tourism); the melting of glaciers also
41 increases the occurrence of glacial disasters, such as glacial lake outburst flooding,
42 icefalls and glacial debris flows (Hock et al., 2019).

43

44 So far, there are not so many approaches used in practice for reducing the rate of
45 glacier ablation. Some technical measures, including energy conservation,
46 temperature-increase control and establishing glacial reserves, have been taken to
47 reduce the ice melting on Earth. In recent years, new ideas and techniques have
48 emerged for slowing the melting of glaciers. For example, in the Rhone glacier of the
49 Swiss Alps, white blankets are used to shelter the glacier and slow down its melting
50 (Dyer, 2019). In the Morteratsch Glacier of the Alps, artificial snow was expected to
51 be applied for slowing down the glacier melting (Oerlemans et al., 2017). In Austrian
52 glacier ski resorts, over 20-m thickness of the ice was preserved on mass balance
53 managed areas compared to non-maintained areas during 1997 – 2006 (Fischer et
54 al., 2016).

55

56 Cloud-seeding over a glacier to generate and enhance snowfall for reducing mass
57 loss has rarely been tested in previous study. There have always been controversial
58 discussions on the virtual efficacy and positiveness of using AgI smoke to seed cloud
59 and enhancing precipitations since the measure was introduced by Vonnegut (1947).
60 The controversy mainly resides in two sides. One side claimed that no statistical or

61 physical evidence had been provided to establish the scientific validity of the
62 operations (Council, 2003; Silverman, 2001), while the other affirmed that the past
63 operations conducted in Australia successfully increased precipitations by 5% up to
64 50% (Bowen, 1952; CSIRO, 1978; Smith, 1967). However, both sides agreed that
65 the experiments of seeding clouds and producing more precipitation were promising
66 and deserved more observations to understand the link of physical reactions leading
67 to precipitation (Council, 2003). A peer review report on global artificial-snowfall
68 activities by the World Meteorological Organization suggests that the toxicity of the
69 seeding material (majorly silver iodine, i.e. AgI) is unlikely to trigger environmental
70 hazards (Flossmann et al., 2018). A potential concern is that artificial-precipitation
71 activities might redistribute the natural precipitation over a region; however, applying
72 cloud seeding over the mountain glaciers usually up to 5 km in length in Central
73 Asia, is presumably acceptable.

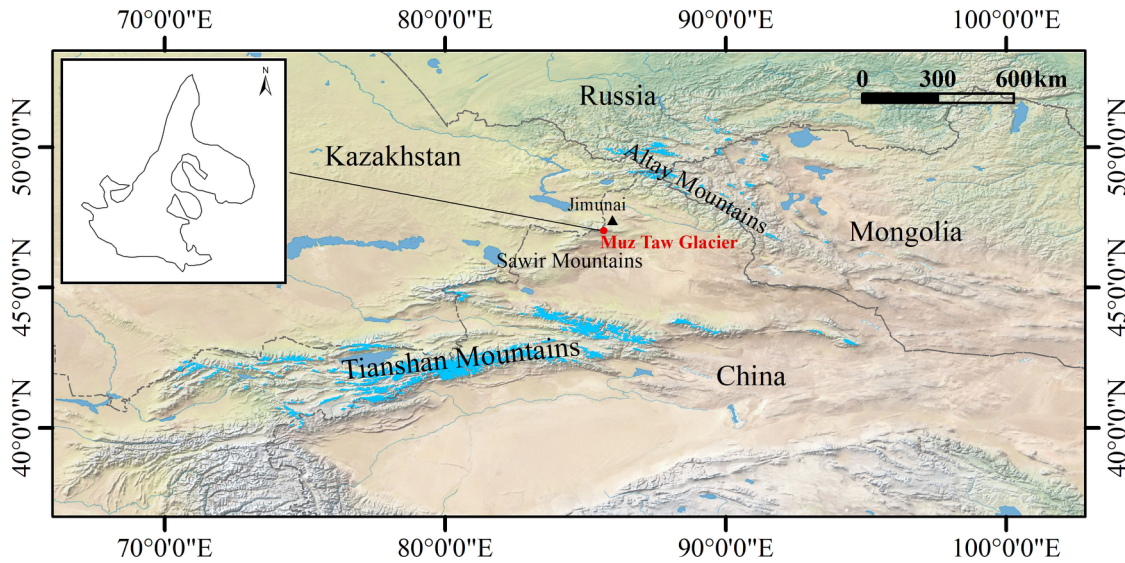
74

75 As an attempt, we select the Muz Tau glacier in the Sawir Mountains as the
76 projected glacier. During the glacier's ablation period in 2018, we tried to induce
77 artificial precipitations by using the ground AgI smoke generators to seed clouds
78 over the glacier. These smog generators were set up there by the local
79 meteorological service for artificial-precipitation tasks. We also combined the
80 precipitation amounts and type, time and frequency recorded by the rainfall gauge
81 and the mass balance and albedo of the glacier measured to study the role of
82 artificial snowfall in reducing the mass loss of the glacier.

83

84 **2 The Sawir Mountains and the Muz Taw Glacier**

85 The Sawir Mountains span the border shared by China and Kazakhstan and are the
86 transitional section between the Tianshan Mountains and the central Altay
87 Mountains. The Muz Taw Glacier (47°04'N, 85°34'E) is a northeast-orientated valley
88 glacier with an area of 3.13 km² and a length of 3.2 km in 2016, located on the
89 northern side of the Sawir Mountains (Figure 1). Its elevation from the terminus to
90 the highest point ranges from 3137 m to 3818 m a.s.l. and its ice volume is 0.28 km³,
91 with an average ice thickness of 66 m (Wang et al., 2018).



92

93 *Figure 1 Location of the Muz Taw glacier and the Sawir Mountains, where the map in the background*
 94 *is downloaded from the website <https://www.naturalearthdata.com/> and the outline of the glacier is*
 95 *sourced in Guo et al. (2015).*
 96

97

98 The general circulation over the study area is featured by the prevailing westerlies
 99 interacting with the Asian anticyclone and polar air mass in winter (Panagiotopoulos
 100 et al., 2005). At the Jimunai Meteorological Station (984 m a.s.l.), 46 km northeast of
 101 the Muz Taw Glacier, the annual mean air temperature measured was 4.27 °C; the
 102 annual mean precipitation was 212 mm during 1961–2016, and the winter
 103 precipitation accounted for 10% - 30% of the annual total.

104

105 The Muz Taw Glacier has been in constant recession since 1959 (Wang et al.,
 106 2019). Especially for the past 20 years, it has been experiencing a rapid and
 107 accelerated shrinkage. From 1977 to 2017, the glacier area decreased by 10.51 km²,
 108 accounting for 45.72 % of its previous surface area (Wang et al., 2019). The average
 109 retreat rate of the glacier terminus was 11.5 m a⁻¹ during 1989 – 2017. The latest
 110 measurements show the mass balance of the Muz Taw Glacier was – 975 mm w.e.
 111 in 2016, – 1192 mm w.e. in 2017 and – 1286 mm w.e. in 2018, respectively; and the
 112 annual equilibrium line of the glacier was approximately 3400 m a.s.l. (Song, 2019).

113

113 **3 Field Experiments and measurements**

114 **3.1 Meteorological radar observations**

115 We used a WR-08X digital radar system (Wuxi Leyoung Electronics Technology Co.,
 116 Ltd) built up at the Jimunai Meteorological station to identify the precipitation clouds

117 around the Sawir Mountains. The radar is a new X-band digital weather radar
118 capable of detecting meteorological targets within 300 km. The radar can
119 quantitatively detect the spatial distribution of intensity of cloud rain targets below 20
120 km distanced from 5 km to 150 km and their motions (e.g., developing height,
121 moving direction and speed.). It can also provide real-time meteorological
122 information. A more detailed description of its application in this area can be referred
123 to in Xu et al. (2017).

124

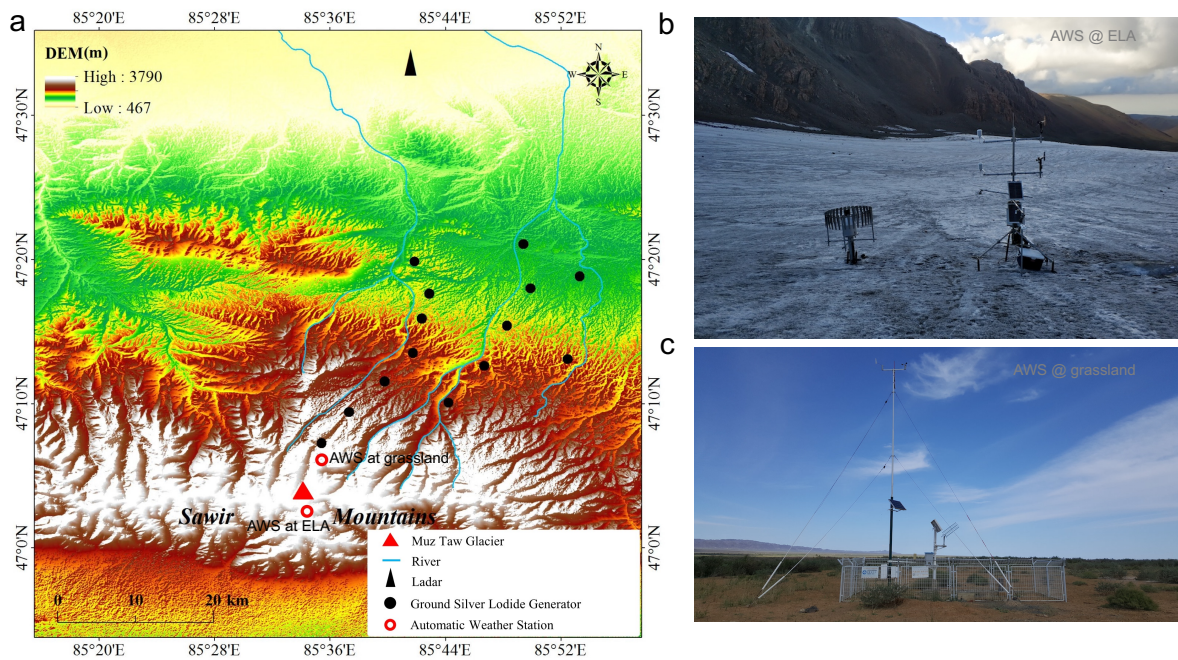
125 **3.2 Artificial-precipitation experiment**

126 The Muz Taw glacier is developing along the valley, and the terminal is the heading
127 source of the Ulequin Urastu River and Ulast River. Fourteen silver-iodide (AgI)
128 smog generators have been distributed along the rivers for artificial-precipitation
129 tasks by the local meteorological service. These smog generators use solar power to
130 light and are remotely controlled. The AgI sticks used in the generators allow to
131 generate 10^{14} AgI-contained ice nuclei per gram at $-7.5\text{ }^{\circ}\text{C} \sim -20\text{ }^{\circ}\text{C}$ (Kong et al.,
132 2016). In the daytime, valley winds prevail along the valley up to the glacier due to
133 intense radiation and the heating-and-lifting effect for air over the snow surface. It is
134 ideal for generating AgI smogs and carrying them by the upwards air stream over the
135 glacier surface to form precipitations. No extra water is needed to form precipitations
136 in our experiments. We monitored the distribution and structural developing of clouds
137 and identified the orientation, height and distance of the clouds approaching the
138 glacier at the radar station. Associated with observing the moving of the potential
139 target clouds and the receiving of the reflection of the radar transmission, we ignited
140 the smog generators for seeding artificial precipitations, when we realized the
141 possibility is high enough to form precipitation potentially (Figure 2). The detailed
142 operation of conducting artificial precipitations in the studied glacier has been
143 described in Xu et al. (2017).

144

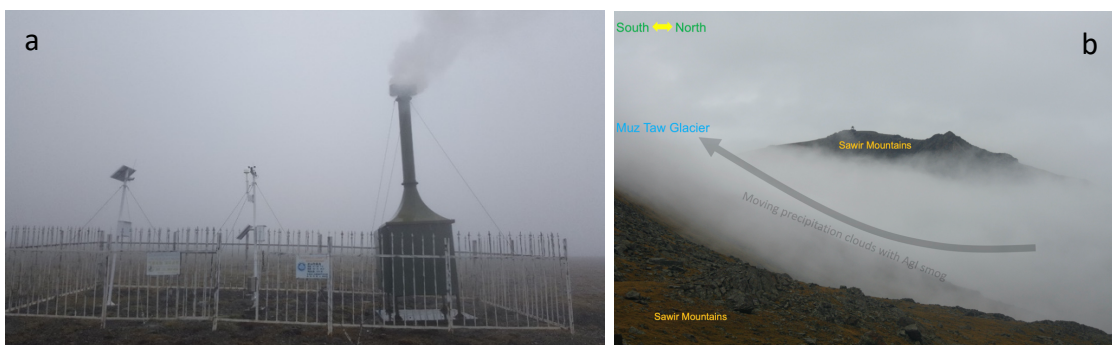
145 First, we used the radar to identify local convective clouds in the background
146 synoptic clouds and measured the orientation, height and distance of the
147 convections for determining the time and area for performing artificial precipitation
148 seeding. And then we chose most favourable timing to ignite the silver-iodide smog
149 generators (Figure 3a) and let the silver-iodide (AgI) particles as catalyzer help

150 forming amounts of artificial ice nuclei (Figure 3b) to absorb more water vapour and
 151 promote to form precipitations.



152
 153 *Figure 2 a) The map of the study area, including the Muz Taw glacier, the two automatic weather*
 154 *stations (AWS) set up at the equilibrium line elevation (ELA) and the forefield of the glacier and the*
 155 *distribution of the silver-iodide-smog generators along the Ulequin Urastu River and Ulast River in the*
 156 *Sawir Mountains for seeding artificial precipitations, b) the AWS set up at ELA and c) the AWS set up*
 157 *at grassland with a straight distance of ~5 km north to the AWS at ELA.*

158



159
 160 *Figure 3 a) Igniting the AgI smog generators along the terminal river when the cloud accumulated late*
 161 *on the afternoon of 19 and 22 Aug 2018, and b) the accumulating of clouds in the valley of the Muz*
 162 *Taw Glacier favoured by the AgI particles moved up towards the summit of the glacier.*

163

164 **3.3 Measurement by the automatic weather stations (AWS)**

165 We set up an automatic weather station (AWS at ELA) on a relatively flat surface
 166 near the equilibrium line altitude (ELA) of the Muz Taw glacier since 8 Aug 2018 (47°
 167 03'36"N, 85°33'43"E, 3430 m a. s. l.; Figure 2a&b and Figure 4). The AWS has

168 various sensors to fulfil the requirement of our study (Table 1). A thermometer
 169 (Pt100 RTD, ± 0.1 K) was mounted horizontally 1.5 m above the surface to measure
 170 air temperature. The measurement of albedo was calculated by measuring incoming
 171 and reflected shortwave radiation with the CNR4 pyranometer mounted on the AWS
 172 at the height of 1.5 m. The error of pyranometer is smaller than 1% in the wavelength
 173 from 0.3 μm to 2.8 μm . Precipitation was measured by an auto-weighing gauge (T-
 174 200B, Geonor Inc.) with an accuracy of about $\pm 0.1\%$. All sensors were connected to
 175 a data logger (CR6, Campbell) which is able to work in low temperature (-55 °C) and
 176 record the hourly means every ten seconds. In the forefield of the glacier around five
 177 kilometers north of the AWS at the ELA, another AWS on the grassland (AWS at
 178 grassland) was set up by the local meteorological service to monitor conventional
 179 meteorology (Figure 2a&c).

180

181 *Table 1 The sensors mounted on the AWS at ELA and their technic features*

Sensor	Measurement	Model	Accuracy or features
Thermometer	temperature	Pt100 RTC	± 0.1 K
Pyranometer	radiation	CNR4	< 1% in 0.3 - 2.8 μm
Auto-weighing gauge	precipitation	T-200B, Geonor Inc.	$\pm 0.1\%$
Data logger	data recording	CR6, Campbell	working in low temperature

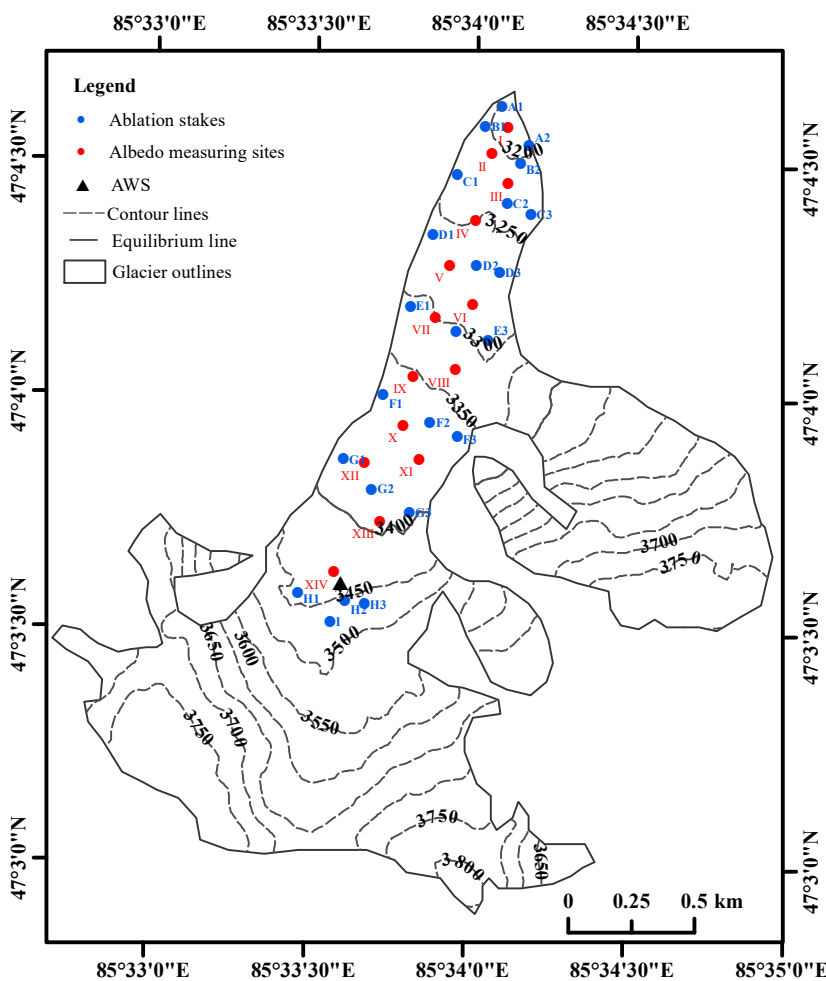
182

183 **3.4 Measurement of the surface spectral reflectance**

184 We used an ASD Fieldspec HandHeld 2 Spectroradiometer to measure the
 185 reflectance data at 325-1075 nm by with a resolution of 3 nm and an error of less
 186 than 4%. The measurement sensor fitted with a bare fibre was mounted on a tripod
 187 at 0.5 m above the surface and had a 25° field of view to a spot sized ~ 0.225 m in
 188 diameter. The spectroradiometer was calibrated to hemispherical atmospheric
 189 conditions at the time, by viewing white-reference panel and then viewing the glacier
 190 surface. We recalibrated the instrument on occasion when the sky radiation
 191 conditions changed. To minimize the influence of slope and solar zenith angle on
 192 albedo, we conducted the measurements in a water-level plane within 12:00-16:00
 193 local time. At each sampling site, three consecutive spectra consisting of ten dark
 194 currents per scan and ten white reference measurements were recorded and
 195 averaged. Meanwhile, cloud cover and surface type were noted for each
 196 measurement.

197

198 We measured spectral reflectance at fourteen sites across the glacier, on 18, 20, 22
 199 and 24 Aug 2018 (Figure 4). In house, the spectrum data were exported from the
 200 instrument by the Spectral Analysis and Management System software (HH2 Sync).
 201 The broadband albedo was calculated as a weighted average based on the spectral
 202 reflectance and the incoming solar radiation across the entire spectral wavelengths
 203 at each site (Ming et al., 2016; Moustafa et al., 2015; Wright et al., 2014; Yue et al.,
 204 2017). The period-mean albedo averaged for the 14 sites before and after
 205 conducting artificial-precipitation experiments (12 – 18 Aug and 18 – 24 Aug) are
 206 shown in Table 2. We excluded the apparent outliers (higher than 0.98) of the albedo
 207 data which are physically unrealistic.



208
 209 *Figure 4 The location of the AWS at ELA and the measuring sites for surface albedo and mass*
 210 *balance on the Muz Taw glacier.*
 211

212 3.5 Measurement of the mass balance

213 We have measured the mass balance of the Muz Taw Glacier annually since 2014
 214 with the method introduced in Østrem and Brugman (1991). Metal stakes for mass-

215 balance measurements were fixed into the ice with a portable steam drill. The stake
216 network consisted of 23 stakes evenly distributed in different altitudes, where three
217 stakes in every row roughly (Figure 4). The stick scale for measuring balance was
218 read thrice, 12, 18 and 24 Aug, respectively. We compared the mass varying
219 between the two periods (12-18 Aug and 18-24 Aug). The snow depth at each stake
220 was measured by reading the scale, and the density of snow was measured by
221 weighing the mass of snow with a given volume. We used the depth and density
222 data of snow to calculate the mass balance at the stake sites. The mass balance
223 was obtained on 1 May and 31 Aug annually. For verifying the effect of artificial
224 snowfalls on the mass balance of the glacier, in particular, we conducted three
225 additional measurements for the mass balance on 12, 18 and 24 Aug 2018,
226 respectively. The baseline of all the mass balance data in this study is the mass
227 balance measured by the stakes on 12 Aug. The calculation of the mass balance of
228 the whole glacier is following an interpolated method based on singular-point
229 measurements introduced by Wang et al. (2014).

230

231 **4 Results and discussion**

232 **4.1 Natural or artificial precipitations and their amounts and forms**

233 Figure 5a shows the hourly temperature and precipitations recorded by the AWS at
234 ELA from 12 to 24 Aug 2018. There were some natural precipitations during 12 – 14
235 Aug, while except this and that in the experiment days, the whole period of 12 – 24
236 Aug was sparse in precipitations. Artificial-precipitation experiments were carried out
237 on 19, 22 and 23 Aug. The precipitation rates on 19th, 20th, 22nd and 23rd were 6.2,
238 1.3, 1.8 and 10.6 mm/day, respectively. Most snowfalls were observed during
239 midnights and early mornings. It seems not likely to distinguish the artificial
240 precipitations from the natural ones if they were simultaneously mixed in all these
241 events.

242

243 Previous weather modification experiments using the same method as ours
244 concluded that it was challenging to tell that how much artificial precipitation mixed in
245 the whole amount directly came after conducting the cloud seeding (CSIRO, 1978;
246 Qiu and Cressey, 2008; Ryan and King, 1997). The results from the measurements
247 by Marcolli et al. (2016) and (Fisher et al., 2018) suggested the efficacy and success
248 of using AgI on growing ice nuclei in clouds and promoting snowfall. In our study,

249 there were significant precipitation amounts recorded by the AWS at ELA every
250 single time after we ignited the smoke generators, associated with a highly
251 significant linear relationship ($n = 10$, $r^2 = 0.9999$) between the timings of igniting Agl
252 and recording snowfalls (Figure 5b). The co-occurring of the significant snow falling
253 using the Agl smoke to seed cloud (Figure 3 and Figure 5b) allows supposing that
254 we were producing artificial precipitations.

255

256 The AWS at grassland in the forefield of the Muz Taw glacier was clear from the Agl
257 smoke during the AP experiments. This allows us to use the precipitation data
258 recorded by it as a control to distinguish natural precipitation from the artificial
259 recorded by the AWS at ELA. We lost the precipitation data from the AWS at
260 grassland during the first AP experiment on Aug 19 for the rain gauge was full and
261 overflowed. While for the second experiment, the precipitation data were
262 successfully collected from the AWS at grassland for a comparison.

263

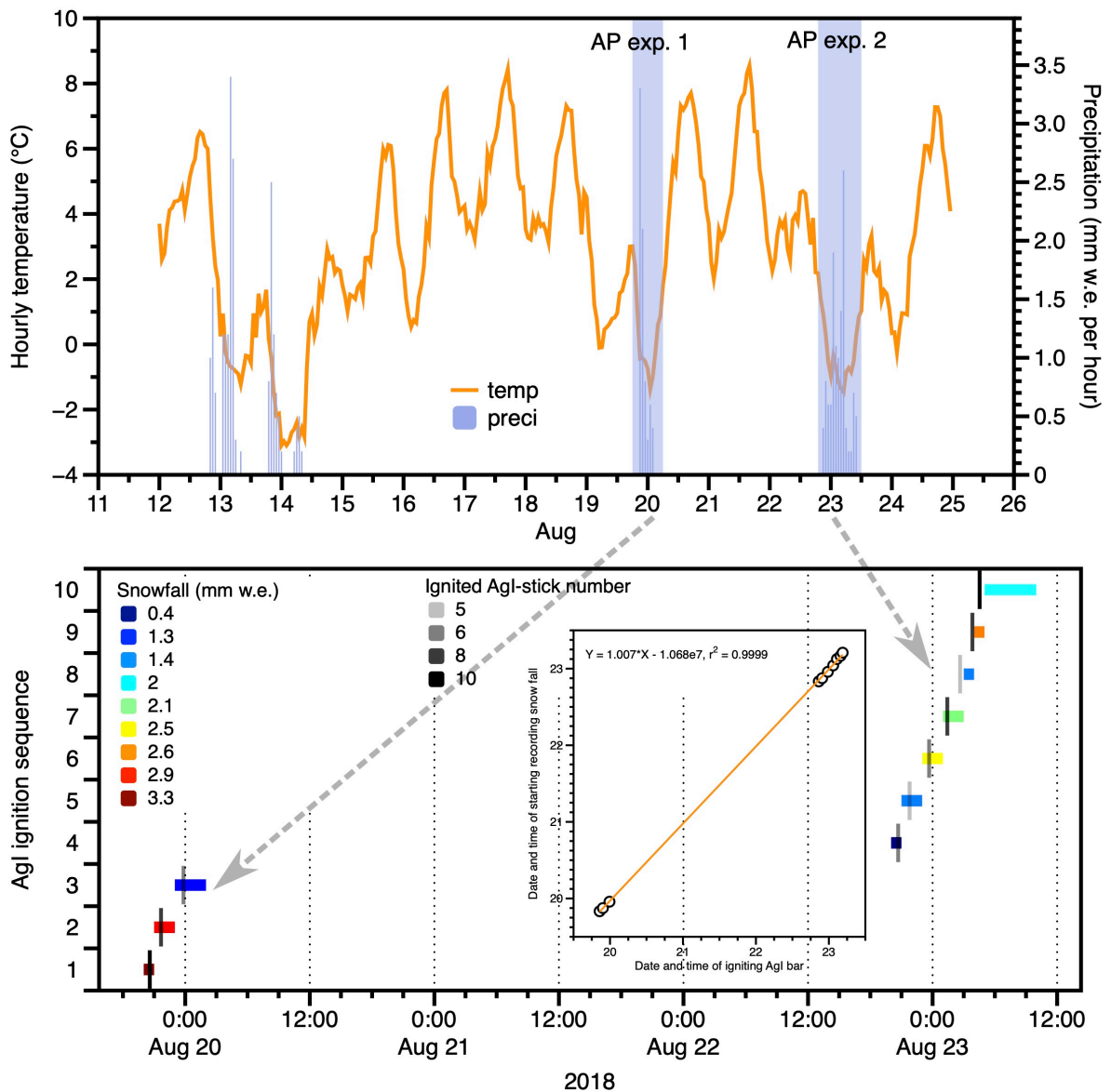
264 Figure 6 shows the precipitations recorded by both AWSs and the record ratio of
265 grassland to ELA during the second AP experiment (Aug 22 to 23). The
266 precipitations recorded by the two AWSs were not synchronized. The AWS at ELA
267 did not record any precipitations when that at grassland recorded at 19:00 and 20:00
268 on Aug 22; while there were records after 6:00 by the AWS at ELA but none for at
269 grassland. The correlation between the two precipitation records is fairly weak ($r^2 =$
270 0.05) when they were both recorded by the AWSs, implying that the cause of
271 precipitation (i.e. natural or artificial) might be distinctly different or likely mixed on
272 the target area.

273

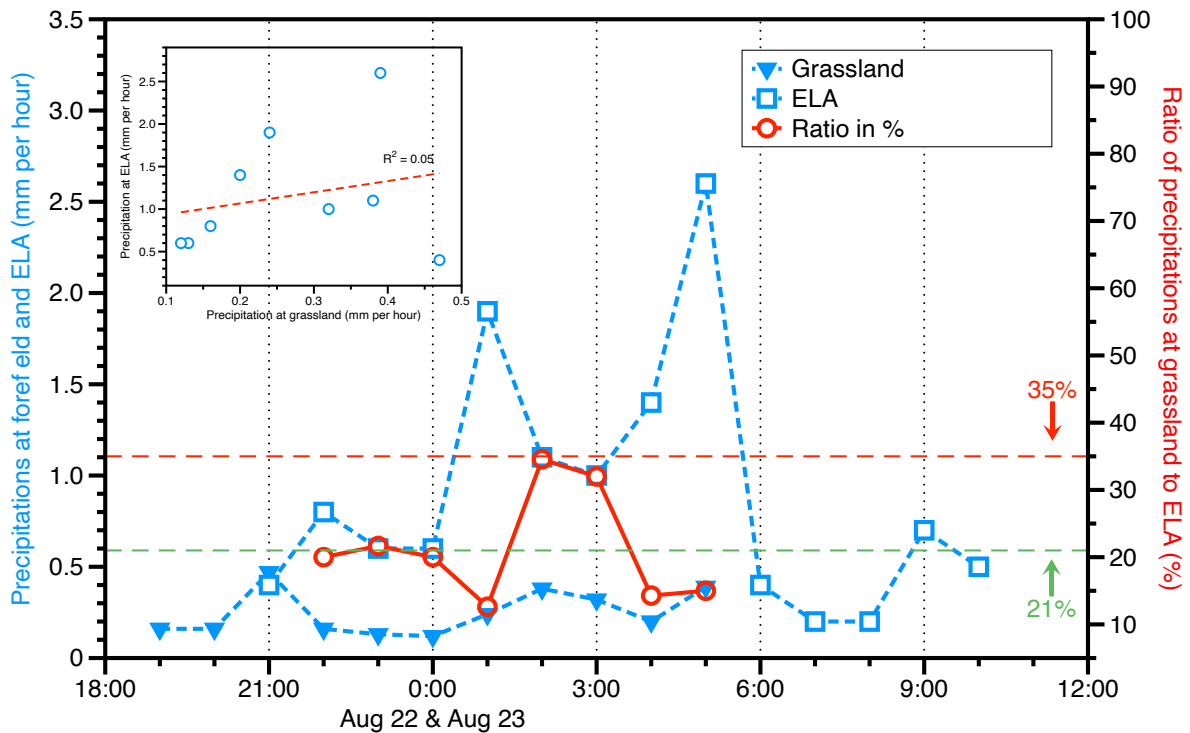
274 We presume two possibilities of whether there was natural precipitation joined the
275 artificial process targeted on the glacier. The first was none natural precipitation took
276 part in conceiving artificial snow on the target area, and the second, if any, was a
277 part of this. The ratios of precipitations by the AWS at grassland to that at ELA were
278 smaller than 35% with a mean of $21 \pm 3 \%$ (Figure 6), which could be used for
279 estimating how much naturally induced precipitation taking part in the AP experiment
280 based on the second presumption.

281

282 To determine the amount of solid precipitations that accumulates on the glacier
 283 surface, we apply a sinusoidal function (Möller et al., 2007) on the total precipitation.
 284 The function describes the transition between solid and liquid precipitations in a
 285 temperature range between +2 °C and +4 °C (Fujita and Ageta, 2000; Mölg et al.,
 286 2012). When the air temperature is lower than 2 °C, solid precipitations (snow) will
 287 occur, and between 2 – 4 °C rain would fall with snow. During our experiments, the
 288 air temperatures were below 2 °C when precipitations occur, implying that the
 289 precipitations in the two experiments were solid.



290
 291 *Figure 5 a) The daily snowfalls and hourly averaged temperature recorded by the AWS at ELA from*
 292 *12 to 24 Aug 2018, where the two artificial-precipitation experiments (AP exp. 1 and 2) are marked,*
 293 *and b) the hourly snowfall amounts (indicated by color) and time periods (indicated by length)*
 294 *recorded by the AWS at ELA and the ignited Agl-stick number (indicated by color) and time during the*
 295 *two experiments.*



296

297 *Figure 6 The precipitations recorded by the AWSs at grassland (inversed blue solid triangles) and*
 298 *ELA (hollow blue squares) and the precipitation-record ratio of grassland to ELA (hollow red circles)*
 299 *during Aug 22 to 23, in which the scatter plot of the precipitations by both AWSs is included and the*
 300 *green and red dashed lines indicate the upper limit and mean of the ratios.*

301

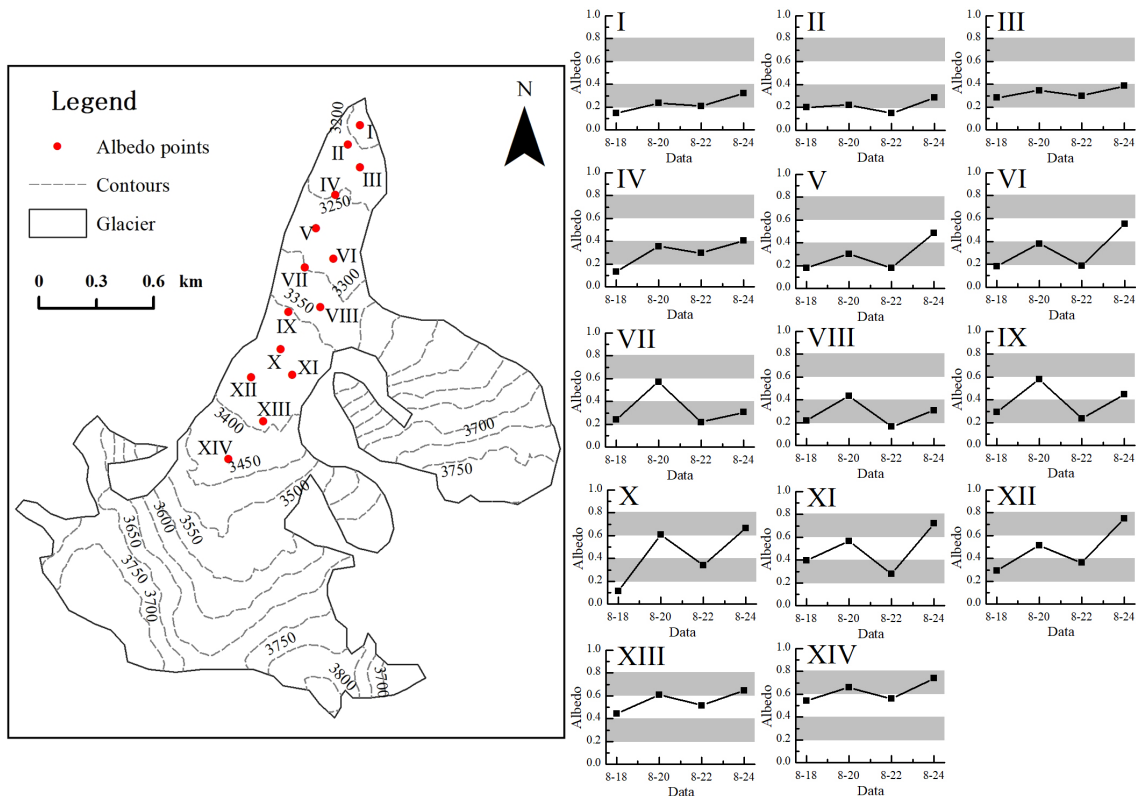
302 **4.2 The effects of artificial snowfall on surface albedo**

303 Glacier albedo is highly sensitive to snowfall. Once a snowfall occurs, it will quickly
 304 whiten the surface of the glacier and increase the albedo. Figure 7 shows the
 305 surface albedo of the Muz Taw Glacier at different locations before and after the
 306 artificial-snowfall experiments. We observed that the surface albedo at the sites
 307 varied from relative flatness (e.g., at site I and site III) to more significant fluctuations
 308 (e.g., at site XII and site VII) between 18 and 24 Aug.

309

310 Below 3250 m, the surface albedo (at sites I, II, III and IV) was generally smaller than
 311 0.4 (typical albedo of ice with debris) with mild fluctuations as shown in Figure 7.
 312 From 3250 to 3350 m a.s.l. (at sites V, VI, VII and VIII), significant variations in
 313 albedo were observed, ranging from 0.2 to 0.6. In the area of 3350-3400 m a.s.l.,
 314 more significant variations in albedo were observed between 0.1 and 0.7. Because
 315 this area was located near the equilibrium line, it was highly sensitive to air
 316 temperature and snowfall. Artificial snowfall frequently transited the surface from ice

317 to snow, and air temperature turned the surface inversely from snow to ice, and thus
 318 dramatic changes in albedo occurred. At sites XIII and XIV, which are much higher
 319 than the equilibrium line, the overall albedo exceeded 0.4 and rose up to 0.8. We
 320 observed a slightly increasing trend in albedo at these two sites (XIII and XIV),
 321 suggesting that the surface was covered by relatively lasting snow owing to artificial
 322 snowfalls.



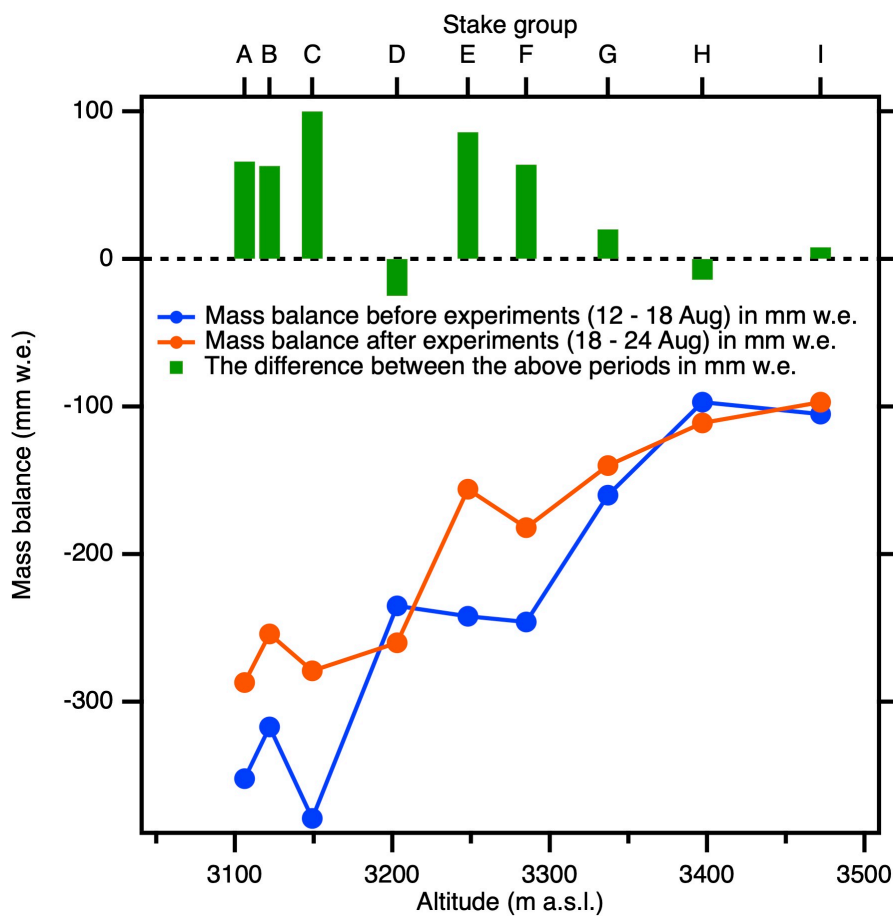
323
 324 *Figure 7 The surface albedo at the fourteen sites (I - XIV) of the Muz Taw Glacier, where the red*
 325 *points denote the sites and the top-left chart as the reference of the fourteen charts (site I to XIV)*
 326 *marks the albedo scale and date with the highlighted grey shades.*

327

328 4.3 The varying mass balance responding to the artificial snowfalls

329 As mentioned in Section 3.4, the stick scale for measuring balance was read thrice
 330 at each site, on 12, 18 and 24 Aug, respectively. To study the effects of the artificial
 331 snowfalls on the mass balance of the glacier, we calculated the mass balance
 332 measured by the stakes during the two periods, i.e. before the artificial snowfalls (12
 333 – 18 Aug) and after the artificial snowfalls (18 – 24 Aug), respectively. The stakes in
 334 a group (A to I) were roughly along the altitude contour (Figure 4), and the
 335 correspondingly measured mass balance of the same group was averaged (Figure
 336 8). The mass balance decrease with altitude from approx. – 400 mm w.e. at 3100 m

337 to approx. – 100 mm w.e. at the equilibrium line measured by the stakes before the
 338 artificial snowfalls, and decrease from approx. – 300 mm w.e. at 3100 m to approx. –
 339 100 mm w.e. at the equilibrium line after the artificial snowfalls. The difference of the
 340 mass balances measured at the sites between the two periods was 41 ± 15 mm w.e.
 341 averaged on the stake measurements for the Muz Taw Glacier, considering the
 342 difference was completely due to artificial precipitation. If we take 21% of the
 343 difference was due to natural precipitation (Figure 6), the difference would be 32 mm
 344 w.e. Therefore, the difference resulting from the artificial snowfalls accounted for
 345 between 14% (with 21% natural) and 17% (without natural) of the mass balance
 346 before the artificial snowfalls (- 237 mm w.e.).



347
 348 *Figure 8 The averaged mass balance measured at the sites (Stake A - I) before (blue) and after*
 349 *(orange) the artificial snowfalls on 18 and 20 Aug compared with that on 12 Aug (The zero line), and*
 350 *the gained mass (green = orange - blue) due to the artificial snowfalls.*

351

352 We compare the positively accumulative temperatures (in brief $PAT = \sum_{i=1}^n T_i$, n is
 353 the number of days, and T is the daily averaged temperature in °C), the amounts of
 354 snowfalls, and the surface albedo of the measurements from 12 to 18 Aug (t_1) and

355 from 18 to 24 Aug (t_2) (Table 2), respectively. The two periods represent the same
 356 time-length span before and after the artificial snowfalls, respectively. The
 357 temperature, snowfall and albedo data in this comparison are all from the
 358 measurements of the AWS at ELA. The estimated mass balance after interpolating
 359 the measured mass balance by the stakes to the whole glacier during t_1 and t_2 were
 360 – 61.4 mm w.e. and – 37.2 mm w.e., respectively. Although the PAT was higher
 361 during t_2 than during t_1 , the mass loss of the glacier was 40% lower than t_1 . More
 362 snowfall and higher albedo resulting from the artificial snowfalls can explain the
 363 lower mass loss during t_2 .

364

365 *Table 2 The positive accumulated temperatures, snowfalls and albedo measured by the instruments*
 366 *on the AWS at ELA, and the calculated mass balances of the Muz Tau glacier before and after the*
 367 *two artificial-snowfall experiments ($t_1 = 12 - 18$ Aug, and $t_2 = 18 - 24$ Aug).*

Period	Positively accumulated temperature (°C)	Snowfall (mm w.e.)	Albedo	Mass balance (mm w.e.)
t_1	17.0	17.4	0.24	- 61.4
t_2	18.2	19.9	0.33	- 37.2

368

369 The accumulation at the equilibrium line altitude (ELA) of a glacier is approximately
 370 equal to the area average of accumulation over the whole glacier (Braithwaite,
 371 2008). We can presume that the snowfall amount measured by the AWS at ELA of
 372 the Muz Tau glacier during t_2 was the average received mass of the whole glacier
 373 after implementing the AP experiments. The extra melt amount from the glacier
 374 besides the gained mass during t_2 would be the difference between the calculated
 375 mass loss (37.2 mm w.e.) and the snow mass measured by the AWS at ELA (19.9
 376 mm. w.e.), and that would be 17.3 mm w.e. The artificial snowfalls may significantly
 377 save the melt of the glacier by 54% during t_2 , calculated as the percentage of the
 378 snowfall divided by the estimated mass balance. Excluding 21% of the mass
 379 measured by the AWS at ELA presumably as the contribution of natural
 380 precipitations, we conclude that the artificial precipitations buffered the total melting
 381 during t_2 by 42%.

382

383 **4.4 The mechanism: how artificial snowfalls reduce the melting of a glacier**

384 In the air temperature lower than 2 °C, the artificial snowfall promotes the form of
385 snow which directly adds mass onto the glacier and increases the mass balance of
386 the glacier and thereby albedo; the snow cools the surface and increases the surface
387 albedo; the increased albedo will decrease the solar radiation absorption in the
388 surface and favour retaining the mass which will, in turn, save the albedo; and
389 eventually the whole process forms a positive feedback.

390

391 This is a very preliminary theory based on the limited data derived from the short-
392 term experiments, and we need further studies to validate the theory. The albedo
393 decay of artificial snowfall and snow physics are required to claim a long-term impact
394 on the mass balance of glaciers. Particularly, the variation in the likelihood of a
395 snowfall event occurring with or without smoke generators and the partition of natural
396 and artificial precipitations need to be quantified more confidently, for which more
397 controlling experiments are needed in future.

398

399 **5 Conclusions**

400 We used Agl-smoke generators to induce artificial snow on the Muz Taw Glacier in
401 Sawir Mountains on 19 and 22 Aug 2018. Two AWSs were set up on the target
402 glacier and control area, respectively. The albedo and mass balance were measured
403 at the stakes evenly distributed along the altitude contours of the glacier before and
404 after the artificial snowfall experiments. The glacier received a total snow amount of
405 ~ 20 mm w.e. by two experiments, which increased the surface albedo of the glacier.
406 Larger fluctuations in albedo were measured at the higher sites than lower.

407

408 By comparing the precipitations measured by the two AWSs, we conclude that
409 artificially induced snow could account for at least 79% of the total snow measured
410 by the AWS at ELA. After interpolating the mass balance measured by the stakes to
411 the whole glacier, we get a mass balance of – 61 mm w.e. for the period of 12 – 18
412 Aug and – 37 mm w.e. for the period of 18 – 24 Aug, respectively. The artificial snow
413 reduced the mass loss of the glacier by ~ 40% due to more snowfall and higher
414 albedo, nevertheless the positively accumulated temperature during the latter period
415 was higher than the former.

416

417 We compared the mass balances directly calculated from the measurements of the
418 stakes before the experiments (12 – 18 Aug) with that after (18 – 24 Aug). The
419 difference between the two periods was between 32 and 41 mm w.e., taking possible
420 natural snow into account. This suggests that artificial snow does add mass to the
421 glacier, which is consistent with the result by interpolating stake measurements to
422 the whole glacier. We also compared the total melt of the glacier during 18 – 24 Aug
423 with the artificial snow received by the glacier, implying that artificial snow
424 significantly saved the mass loss by between 42% and 54% after the experiments.

425

426 We propose a theory describing the role of snowfall in reducing the melting of the
427 glacier. The mechanism determines that the environmental temperature and the form
428 of snowfall, and clouds are the two main factors resulting in the mass gain and loss
429 of a glacier. Mechanical erosion, energy exchange (thermal-dynamic) and albedo-
430 induced radiation absorption play major roles in the process of mass varying. This
431 hypothesized mechanism is preliminary and needs more measurements to
432 consolidate.

433

434 The approach in our work uses solar power to ignite the seeding material for forming
435 clouds and uses no extra water but redistributes natural water in the local
436 atmosphere at a small spatial scale. The energy-and-water saving techniques of the
437 approach with reasonably mass-loss-reducing efficiency from the Muz Taw glacier
438 validates its efficiency to possibly be applied in more Central-Asian glaciers to
439 reduce their rapid melting. Especially in summer when the melting is dramatic in the
440 Central-Asian glaciers, applying the approach suggested by our study on a much
441 broader scale might reduce the melting significantly. However, it is important to note
442 that our approach needs a priori atmospheric conditions favourable to precipitation
443 and can not be applied if the weather is dry and sunny. This study is preliminary and
444 short in operating time and needs more sophisticated experiments at control and
445 target areas to partition natural and artificial precipitations. The approach would
446 sophisticate itself when being implemented more regularly in future repeated and
447 longer-term, or scaled-up experiments.

448

449 **Code/Data availability**

450 It is currently shared by communities that the dataset would be publicly available
451 upon acceptance of publication. Please directly contact the corresponding author F.
452 Wang (wangfeiteng@lzb.ac.cn) or the coordinating author J. Ming
453 (petermingjing@hotmail.com) for the data repository and the authors will response
454 accordingly.

455

456 **Author contributions**

457 F.W. conceived the main ideas, designed the experiment and drafted the
458 manuscript. X.Y., L.W., H.L. and Z.D. helped to design the experiment and collect
459 the data. J.M. reanalyzed the data and plots, edit and sophisticated the manuscript.
460 Z.L. helped with the final revision.

461

462 **Competing interests**

463 All contributors declare no competing interests in this work.

464

465 **Acknowledgements**

466 The authors thank Samuel Morin and Suryanarayanan Balasubramanian for their
467 comments which are crucial for improving this work. This research is supported by
468 the Second Tibetan Plateau Scientific Expedition and Research (STEP) program
469 (2019QZKK0201), the Strategic Priority Research Program of the Chinese Academy
470 of Sciences (XDA20040501, XDA20060201), the National Natural Science
471 Foundation of China (41771081), the State Key Laboratory of Cryospheric Sciences
472 (SKLCS-ZZ-2019) and the Key Research Program of Frontier Sciences of Chinese
473 Academy of Sciences (QYZDB-SSW-SYS024).

474

475 **References**

476 Bojinski, S., Verstraete, M., Peterson, T. C., Richter, C., Simmons, A., and Zemp, M.: The
477 Concept of Essential Climate Variables in Support of Climate Research, Applications, and
478 Policy, *B Am Meteorol Soc*, 95, 1431-1443, 2014.
479 Bowen, E. G.: AUSTRALIAN EXPERIMENTS ON ARTIFICIAL STIMULATION OF RAINFALL,
480 *Weather*, 7, 204-209, 1952.
481 Braithwaite, R. J.: Temperature and precipitation climate at the equilibrium-line altitude of
482 glaciers expressed by the degree-day factor for melting snow, *Journal of Glaciology*, 54, 437-
483 444, 2008.
484 Council, N. R.: *Critical Issues in Weather Modification Research*, The National Academies
485 Press, Washington, DC, 2003.

486 CSIRO: Rainmaking; the state of the art. In: ECOS, 1978.

487 Dyer, C.: Now THAT'S a wrap! Swiss glacier is shrouded in UV-resistant blankets to stop it
488 melting in the summer heat. In: Daily Mail, Daily Mail, Online, 2019.

489 Fischer, A., Helfricht, K., and Stocker-Waldhuber, M.: Local reduction of decadal glacier
490 thickness loss through mass balance management in ski resorts, *The Cryosphere*, 10, 2941-
491 2952, 2016.

492 Fisher, J. M., Lytle, M. L., Kunkel, M. L., Blestrud, D. R., Dawson, N. W., Parkinson, S. K.,
493 Edwards, R., and Benner, S. G.: Assessment of Ground-Based and Aerial Cloud Seeding Using
494 Trace Chemistry, *Advances in Meteorology*, 2018, 1-15, 2018.

495 Flossmann, A. I., Manton, M. J., Abshaev, A., Bruintjet, R., Murakami, M., Prabhakaran, T.,
496 and Yao, Z.: Peer Review Report on Global Precipitation Enhancement Activities, 2018. 2018.

497 Fujita, K. and Ageta, Y.: Effect of summer accumulation on glacier mass balance on the
498 Tibetan Plateau revealed by mass-balance model, *Journal of Glaciology*, 46, 244-252, 2000.

499 Guo, W., Liu, S., Xu, J., Wu, L., Shangguan, D., Yao, X., Wei, J., Bao, W., Yu, P., and Liu, Q.: The
500 second Chinese glacier inventory: data, methods and results, *Journal of Glaciology*, 61, 357-
501 372, 2015.

502 Hock, R., Rasul, G., Adler, C., Cáceres, B., Gruber, S., Hirabayashi, Y., Jackson, M., Kääh, A.,
503 Kang, S., Kutuzov, S., Milner, A., Molau, U., Morin, S., Orlove, B., and Steltzer, H.: High
504 Mountain Areas. In: IPCC Special Report on the Ocean and Cryosphere in a Changing
505 Climate, IPCC, New York, 2019.

506 Immerzeel, W. W., Lutz, A. F., Andrade, M., Bahl, A., Biemans, H., Bolch, T., Hyde, S.,
507 Brumby, S., Davies, B. J., Elmore, A. C., Emmer, A., Feng, M., Fernández, A., Haritashya, U.,
508 Kargel, J. S., Koppes, M., Kraaijenbrink, P. D. A., Kulkarni, A. V., Mayewski, P., Nepal, S.,
509 Pacheco, P., Painter, T. H., Pellicciotti, F., Rajaram, H., Rupper, S., Sinisalo, A., Shrestha, A. B.,
510 Viviroli, D., Wada, Y., Xiao, C., Yao, T., and Baillie, J. E. M.: Importance and vulnerability of
511 the world's water towers, *Nature*, doi: 10.1038/s41586-019-1822-y, 2019. 2019.

512 Immerzeel, W. W., van Beek, L. P. H., and Bierkens, M. F. P.: Climate Change Will Affect the
513 Asian Water Towers, *Science*, 328, 1382-1385, 2010.

514 Kong, J., Wang, G., Fang, W., and Su, Z.: Laboratory study on nucleating properties and
515 microstructure of AgI pyrotechnics, *Meteorological Monthly*, 42, 74-79, 2016.

516 Marcolli, C., Nagare, B., Welti, A., and Lohmann, U.: Ice nucleation efficiency of AgI: review
517 and new insights, *Atmos Chem Phys*, 16, 8915-8937, 2016.

518 Ming, J., Xiao, C., Wang, F., Li, Z., and Li, Y.: Grey Tienshan Urumqi Glacier No.1 and light-
519 absorbing impurities, *Environmental science and pollution research international*, 23, 9549-
520 9558, 2016.

521 Mölg, T., Maussion, F., Yang, W., and Scherer, D.: The footprint of Asian monsoon dynamics
522 in the mass and energy balance of a Tibetan glacier, *The Cryosphere*, 6, 1445-1461, 2012.

523 Möller, M., Schneider, C., and Kilian, R.: Glacier change and climate forcing in recent
524 decades at Gran Campo Nevado, southernmost Patagonia, *Annals of Glaciology*, 46, 136-
525 144, 2007.

526 Moustafa, S., Rennermalm, A., Smith, L., Miller, M., Mioduszewski, J., Koenig, L., Hom, M.,
527 and Shuman, C.: Multi-modal albedo distributions in the ablation area of the southwestern
528 Greenland Ice Sheet, *The Cryosphere*, 9, 905-923, 2015.

529 Oerlemans, J., Haag, M., and Keller, F.: Slowing down the retreat of the Morteratsch glacier,
530 Switzerland, by artificially produced summer snow: a feasibility study, *Climatic Change*, 145,
531 189-203, 2017.

532 Østrem, G. and Brugman, M.: Glacier mass-balance measurements: a manual for field and
533 office work, National Hydrology Research Institute, Inland Waters Directorate Conservation
534 and Protection Environment Canada, Saskatoon, Sask, Canada, 224 pp., 1991.
535 Panagiotopoulos, F., Shahgedanova, M., Hannachi, A., and Stephenson, D. B.: Observed
536 Trends and Teleconnections of the Siberian High: A Recently Declining Center of Action, *J*
537 *Climate*, 18, 1411-1422, 2005.
538 Qiu, J. and Cressey, D.: Meteorology: Taming the sky, *Nature*, 453, 970-974, 2008.
539 Ryan, B. F. and King, W. D.: A Critical Review of the Australian Experience in Cloud Seeding,
540 *B Am Meteorol Soc*, 78, 239-254, 1997.
541 Silverman, B. A.: A Critical Assessment of Glaciogenic Seeding of Convective Clouds for
542 Rainfall Enhancement, *B Am Meteorol Soc*, 82, 903-924, 2001.
543 Smith, E. L.: Cloud seeding experiments in Australia, 1967.
544 Song, L.: Blue book on climate change in China, Center on Climate Change Press, 2019.
545 Vonnegut, B.: The Nucleation of Ice Formation by Silver Iodide, *Journal of Applied Physics*,
546 18, 593-595, 1947.
547 Wang, F., Xu, C., Li, Z., Anjum, M. N., and Wang, L.: Applicability of an ultra-long-range
548 terrestrial laser scanner to monitor the mass balance of Muz Taw Glacier, Sawir Mountains,
549 China, *Sciences in Cold and Arid Regions*, 10, 0047-0054, 2018.
550 Wang, P., Li, Z., Li, H., Wang, W., and Yao, H.: Comparison of glaciological and geodetic mass
551 balance at Urumqi Glacier No. 1, Tian Shan, Central Asia, *Global Planet Change*, 114, 14-22,
552 2014.
553 Wang, Y. Q., Zhao, J., Li, Z. Q., and Zhang, M. J.: Glacier changes in the Sawuer Mountain
554 during 1977-2017 and their response to climate change, *Journal of Natural Resources (in*
555 *Chinese)*, 34, 802-814, 2019.
556 Wright, P., Bergin, M., Dibb, J., Lefer, B., Domine, F., Carman, T., Carmagnola, C., Dumont,
557 M., Courville, Z., and Schaaf, C.: Comparing MODIS daily snow albedo to spectral albedo
558 field measurements in Central Greenland, *Remote Sens Environ*, 140, 118-129, 2014.
559 Xu, Z., Jing, H., Zou, L., and Li, Y.: Application research of type WR-08X digital radar on
560 artificial precipitation in Saur Mountains area, *Jiangxi Science (in Chinese)*, 35, 727-730,
561 2017.
562 Yue, X., Zhao, J. U. N., Li, Z., Zhang, M., Fan, J. I. N., Wang, L. I. N., and Wang, P.: Spatial and
563 temporal variations of the surface albedo and other factors influencing Urumqi Glacier No. 1
564 in Tien Shan, China, *Journal of Glaciology*, 63, 899-911, 2017.
565 Zemp, M., Huss, M., Thibert, E., Eckert, N., McNabb, R., Huber, J., Barandun, M., Machguth,
566 H., Nussbaumer, S. U., Gartner-Roer, I., Thomson, L., Paul, F., Maussion, F., Kutuzov, S., and
567 Cogley, J. G.: Global glacier mass changes and their contributions to sea-level rise from 1961
568 to 2016, *Nature*, 568, 382-386, 2019.